SCIENTIFIC PAPER

Investigation of scatter radiation intensities in the cardiac catheter laboratory: novel versus traditional shielding solutions

Negar Mirjalili[1] · Jason Tse[1] · James A. Crowhurst[2,3] · Rustem Dautov[2,3]

Abstract

A manufacturer has released a novel shielding solution (NSS): Rampart M1128 and claimed that the personal protective equipment (PPE) can be removed. This study investigates the scatter intensities with the NSS or the traditional shielding solutions (TSS) including the ceiling-suspended screen and the tableside lead drape. Isodose maps were generated by two series of measurements with an anthropomorphic phantom using NSS and TSS. Three survey meters were positioned at different heights to measure the scatter intensities at the eye, chest, and pelvic levels. Additional measurements were made at the primary and secondary operators? locations to evaluate the scatter intensities with different clinical projections. For the main operator positions, the isodose maps showed that NSS could result in a scatter dose that reduced by 80% to 95% compared to the same positions with TSS at the eye and chest levels. The corresponding result at the pelvic level was a reduction of 50%. These reductions should be compared to the additional protection by PPE: up to 80% reduction from lead eyeglasses and up to 95% from protective garments. Considering both operators at clinically relevant LAO projections, NSS resulted in scatter dose that was 80% to 96%, 76% to 96% and 25% to 60% lower than those of the TSS at eye, chest and pelvis levels. The protection of NSS is comparable with that of TSS alongside PPE at the eye but not at the chest and the pelvic levels under the setup of coronary angiography.

Keywords Scatter radiation · Radiation safety · Radiation shielding · Occupational exposure

Introduction

Radiation exposure is one of the major occupational hazards in cardiac catheter laboratories [1]. Clinicians including cardiologists, radiographers, and scrub nurses are subject to an increased risk of radiation-associated cancer induction and lens opacity formation by exposure to scatter radiation from the imaged patients. Personal Protective Equipment (PPE), and other fixed shielding equipment such as the ceiling-suspended lead acrylic screen are the most common and best available means to reduce such occupational exposures below the safety limits.

Despite its effective protection, the long-term wearing of protective garments has been associated with quality of life issues such as spinal disc damage among cardiologists [1–4]. Several manufacturers have therefore released novel shielding solutions with the claim that they could eliminate the need for conventional protective garments [5–8]. One novel solution is Rampart M1128 (Vestiva Hills, Alabama, United States) which is a floor-mounted radiation shield consisting of two lead acrylic screens (1 mm lead equivalent) surrounding the patient. A preliminary trial by Scott et al. [8] showed that this novel solution could provide between 60% and 84% more scatter dose reduction to the clinicians compared to the control in which the traditional shielding solutions (TSS), was employed. On the other hand, phantom measurements from the same study showed that the novel solution could result in up to 90% dose reduction.

This study aims to investigate the scatter radiation intensities under the typical setup for coronary angiogram (CA) by employing the NSS: Rampart M1128 and comparing it to

✉ Negar Mirjalili
   negar.mirjalili@gmail.com

1 Biomedical Technology Services, The Prince Charles Hospital, Rode Road, Chermside, Brisbane QLD 4031, Australia

2 Department of Cardiology, The Prince Charles Hospital, Rode Road, Chermside, Brisbane QLD 4031, Australia

3 University of Queensland, St Lucia, Brisbane QLD 4072, Australia

the TSS consisting of the ceiling-suspended screen and the tableside lead drape (Mavig, Munich, Germany). Isodose maps were generated at three heights corresponding to the dose to the eye lens, chest, and pelvic when the two different shielding solutions were employed. Additional investigations were made into the change of scatter intensities at the main operators' locations as a function of clinical projection angles. The outcome of this study will inform the protection efficacy of NSS in comparison to TSS and provide practical recommendations should this novel solution be introduced into clinical practice.

Methods

The isodose maps were generated with 60 measurement points, 50 cm apart, around a fixed fluoroscopy X-ray unit (model: Siemens Artis Q biplane; Siemens Healthcare, Germany). The coordinate system of the maps is illustrated in Fig. 1. Cells E5 and E6 correspond to the locations of the primary and secondary operators, protected by either the NSS or the TSS. An anthrophonic phantom (model: PBU-50; Kyoto Kagaku, Kyoto, Japan), simulating a typical patient of height 165 cm and weight 50 kg, was positioned on the treatment table, and irradiated to produce scatter radiation.

Two series of scatter measurements were performed using the Raysafe X2 survey meter (Fluke Biomedical, Billdal, Sweden), one with NSS and the other with TSS in place (Fig. 2a and b). The calibration of the survey meter covers the standard beam qualities in diagnostic X-rays and is traceable to Physikalisch-Technische Bundesanstalt (PTB) primary calibration laboratory. The air kerma rate measurement accounts for up to 10% uncertainty. The survey meter also has an angular dependency of less than 1% within $\pm 10°$. Three survey meters were positioned at 160 cm, 117 cm, and 72 cm above the floor to respectively measure the scatter intensities at the eye, chest, and pelvic levels. The scatter

intensities, in terms of incident air kerma, were normalized by the kerma area product (KAP) value for each exposure to account for any variations in exposure time.

The clinical setup for CA was used throughout the measurements. This involved a left anterior oblique 30-degree (LAO 30) and no caudal/cranial angulation (CAU/CRA0) projection which is common for CA and provides a moderate amount of scatter radiation. The X-ray field was centered at the heart with a field of view set at 20 cm and a source-to-image distance (SID) of 95 cm (approximately 5 cm above the patient's skin surface). The acquisition protocol used was "Card Coro" (medium dose mode) which has a frame rate of 10 fps and a total exposure time of 10 s. With the above projection, the acquisition parameters selected by the automatic dose rate control (ADRC) were 76 kVp, 0.3 mm Copper (Cu) filtration, 262 mA, and 3.4 ms frame duration.

The NSS was positioned in its 180-degree orientation (Fig. 2a), 2 cm above the patient skin surface in conjunction with the recommended table side drapes and vertical extensions. As per the vendor's recommendation, a small lead sheet (300 mm x 500 mm; 0.5 mm lead equivalent) was placed on top of the phantom's abdomen. The lead sheet was to cover any gaps in the soft shielding of the NSS for extra protection of the operators. The TSS was set up as per normal clinical practice without abdominal shield, with the ceiling-suspended shield and the table drapes on the side of the tabletop with the anthropomorphic phantom on the bed (Fig. 2b).

A subsequent set of measurements were performed to investigate the effect of projection angles on scatter radiation intensities. This consisted of measuring scatter radiation

Table 1 Acquisition parameters selected by the ADRC for additional clinically relevant projections

Projections	Acquisition factors
LAO30 CRA30	76 kVp;427 mA;3.9 ms;0.3 Cu; FOV 20 cm
LAO30 CAU30	78 kVp;428 mA;4.3 ms;0.3 Cu; FOV 20 cm
RAO30 CRA30	76 kVp;301 mA;3.4 ms;0.3 Cu; FOV 20 cm
RAO20 CAU20	76 kVp;262 mA;3.4 ms;0.3 Cu; FOV 20 cm

Fig. 1 Coordination system of the isodose maps. The dimension of each measurement cell is 50 cm x 50 cm. Locations of the NSS, TSS, operators 1 and 2 as well as the tabletop (cells D3 to D8) and X-ray equipment (cells C1 to D2) are illustrated
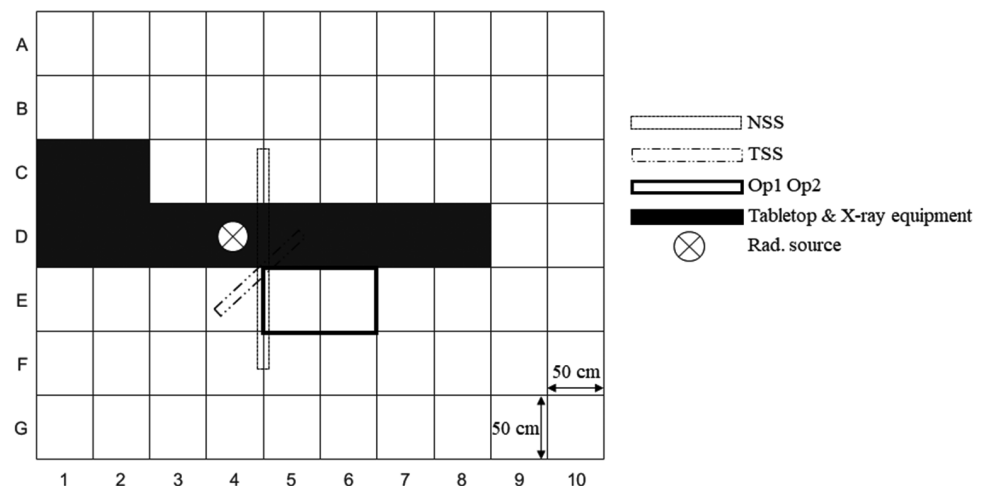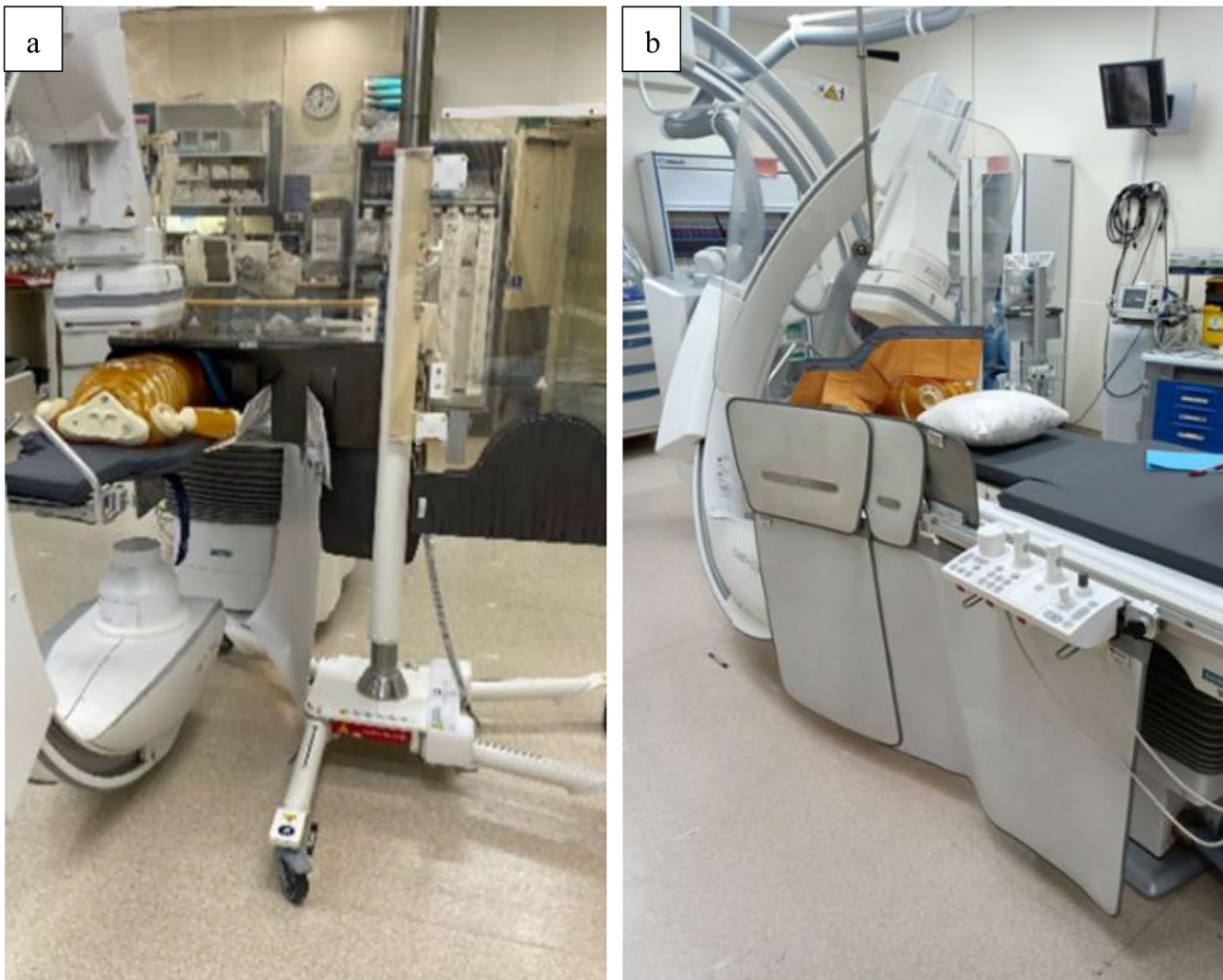
Fig. 2 Measurement setups of **(a)** NSS with table drapes and **(b)** TSS with the anthropomorphic phantom on the tabletop

at the locations of the primary (operator 1) and secondary operators (operator 2) for additional clinically relevant projections of LAO30/CRA30, LAO30/CAU30, RAO (Right Anterior Oblique) 30/CRA30 and RAO20/CAU20, again with 3 survey meters located at the eye, chest, and pelvic levels. The acquisition parameters for those projections are presented in Table 1.

Results

Isodose maps with NSS and TSS

The isodose maps at different measurement heights were illustrated in Fig. 3. Figure 3a, c, e respectively referred to the maps with NSS at the eye, chest and pelvic heights and the corresponding results with TSS are in Fig. 3b, d, f.

NSS is comprised of 1 mm lead equivalence compared to TSS which is 0.5 mm with added protection from PPE. It is worth noting that the results of TSS have not accounted for any protection provided by PPE. For the primary operator (location referred to Fig. 1), NSS resulted in a scatter dose that was around 95% lower than those of TSS, at the eye and chest levels (Eye: NSS 0.6, TSS 13.4 $nGy/\mu Gym^2$; Chest: NSS 0.6, TSS 11.2 $nGy/\mu Gym^2$). At the pelvic level, however, the difference declined to around 60% (Pelvic: NSS 0.2, TSS 0.5 $nGy/\mu Gym^2$). For the secondary operator, the difference was around 80% at the eye and chest levels (Eye: NSS 1.6, TSS 8.1 $nGy/\mu Gym^2$; Chest: NSS 0.9, TSS 4.7 $nGy/\mu Gym^2$) and 50% at the pelvic level (Pelvic: NSS 0.2, TSS 0.4 $nGy/\mu Gym^2$).

Scatter doses were consistently lower at locations E3 and E4 in the isodose maps of NSS compared to those of TSS. This can be attributed to the slightly different positioning of
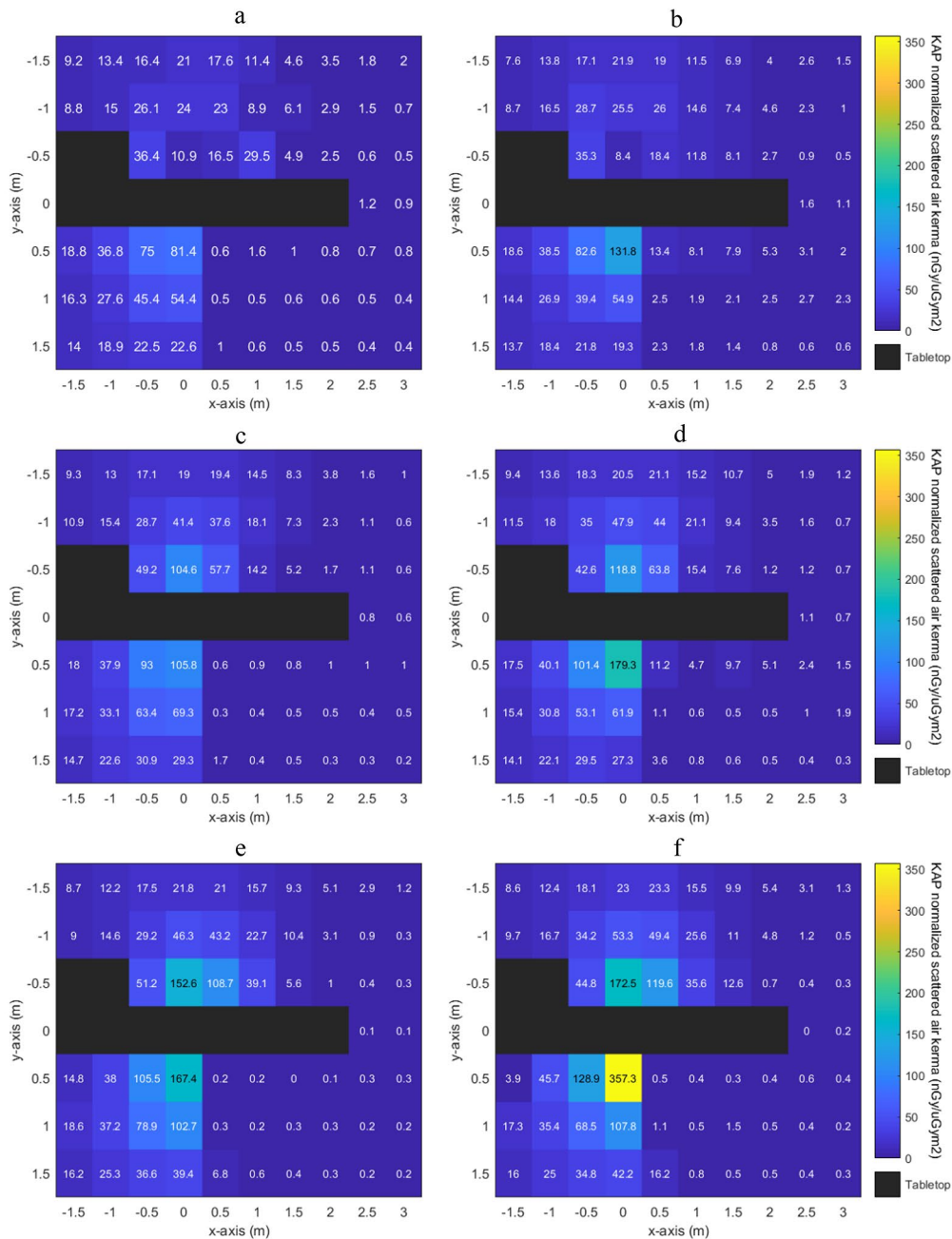
Fig. 3 Isodose maps at the eye, chest, and pelvic levels with NSS **(a, c, e)** and TSS **(b, d, f)**

the survey metres: as shown in Fig. 2a, the base legs of NSS were preventing the survey meters from positioning at the centre of the measurement grid.

Effects of projection angles on scatter radiation intensities

Table 2 showed that the measured scatter intensities with both NSS and TSS would vary with the different projections. Considering both operators at the three LAO30 projections,

NSS resulted in scatter dose that was 80–96% (Eye: NSS 1.6 and 0.6, TSS 8.1 and 13.4 nGy/µGym²), 76–96% (Chest: NSS 0.8 and 0.8, TSS 3.3 and 19.3 nGy/µGym²) and 25–60% (Pelvic: NSS 0.3 and 0.2, TSS 0.4 and 0.5 nGy/µGym²) lower than those of the TSS at the eye, chest and pelvic levels. The difference in protection between the shielding solutions was smaller for the two RAO projections of interest with respective ranges of 48–78% (Eye: NSS 2.2 and 0.8, TSS 4.2 and 3.7 nGy/µGym²), 3–88% (Chest: NSS 3.5 and 0.7, TSS 3.6 and 5.8 nGy/µGym2) and 0–30%

Table 2 Scatter radiation intensities at the primary and secondary operators' locations for various clinical projections

| | | Normalized scatter air kerma (nGy/μGym^2) | | | | | |
		NSS			TSS		
Op 1	Projections	Eye	Chest	Pelvic	Eye	Chest	Pelvic
	LAO30 CRA0	0.6	0.6	0.2	13.4	11.2	0.5
	LAO30 CRA30	1.5	0.8	0.3	9.9	19.3	0.7
	LAO30 CAU30	0.5	1.0	0.5	2.9	5.4	0.8
	RAO30 CRA30	0.8	0.7	0.6	3.7	5.8	0.6
	RAO20 CAU20	0.7	3.5	0.7	2.4	3.6	1.0
Op 2	Projections	Eye	Chest	Pelvic	Eye	Chest	Pelvic
	LAO30 CRA0	1.6	0.9	0.2	8.1	4.7	0.4
	LAO30 CRA30	1.0	0.9	0.3	15.6	13.0	0.4
	LAO30 CAU30	0.9	0.8	0.4	7.8	3.3	0.6
	RAO30 CRA30	2.2	2.2	0.3	4.2	4.4	0.4
	RAO20 CAU20	1.0	0.9	0.4	3.0	5.2	0.4

(Pelvic: NSS 0.4 and 0.7, TSS 0.4 and 1 nGy/μGym^2). In addition, it was observed that certain projections would produce scatter radiation that can "escape" the gaps of a particular shielding solution. For example, RAO20/CAU20 produced an increased scatter dose at the chest level to operator 1 using NSS. This anomalous increase in scatter radiation was not observed in the results of TSS.

Discussion

Our results showed that the protective efficacy of NSS compares favourably with that of TSS alongside PPE at eye level, for most angles at chest levels, but not at pelvic levels. The protection of lead eyeglasses in clinical practice is highly dependent on the clinician's head orientation, design of the eyeglasses, and measurement locations of the eye lens dose [9, 10]. McVey et al. [11] proposed a dose reduction factor of 5 (equating to 80% reduction) for typical eyeglasses of 0.75 mm lead and 0.5 mm lead in the side shields. Another study by van Rooijen et al. [12] reported an average reduction factor of 2.1 (equating to 52% reduction) for the radiologists and eyeglasses models in their study. For comparison, the eye-level isodose maps from this study indicated that NSS could achieve approximately 95% and 80% scatter dose reductions to the primary and secondary operators. Nevertheless, at the chest and particularly the pelvic levels, the dose reductions to the main operators would be lower than those from typical protective garments with lead equivalence between 0.35 and 0.5 mm which can provide around 90% and 95% dose reduction in diagnostic X-ray energies [13]. All in all, the results rebut the claims that NSS alone can provide equivalent protection to TSS alongside the use of PPE.

While the overall protection of NSS may be inferior to TSS with PPE, the solution may permit the use of lightweight protective garments within the "safe zone" in the laboratory (e.g. cells E5:G10 in Fig. 1) as informed by the isodose maps of this work. For ALARA (As Low As Reasonably Achievable), it is recommended that the lead eyeglasses and thyroid shields be used with NSS to further reduce the dose to the eye lens and thyroid, provided that they do not cause significant discomfort to staff. Also, a safety checklist should be implemented to ensure the proper setup of NSS as any gaps between the radiation source and the operators have been shown to compromise its protection.

To the authors' knowledge, this is the first study to thoroughly characterize the scatter intensities in the laboratory when the NSS is in use under clinical setups. Scott et al. [8] also produced preliminary isodose maps for NSS and TSS but only with a standard posterior-anterior (PA) projection which is uncommon in procedures like CA. Our isodose maps also cover the complete layout of the laboratory for the most common CA projection which provides additional dose information and facilitates the correct implementation of the shielding solution.

The present study is subject to several limitations. Firstly, the isodose maps did not consider biplane or cone beam computed tomography imaging which are becoming more common practices in cardiac interventional procedures. Further studies are warranted to study the protective efficacy of NSS for these newer imaging techniques. In addition, exam protocols other than CA may lead to different results due to the difference in the technical factors and clinical projection angles. Lastly, the present study only investigated the scatter radiation intensities around the shielding solutions but did not survey or inform clinicians' experience with the solutions or any practical limitation that it may pose to the clinical procedures (e.g. the use of NSS may limit certain projections alongside the cranial-caudal direction).

Conclusions

The protective efficacy of NSS is comparable with that of TSS alongside PPE at the eye but not at the chest and pelvic levels, under the clinical setup of CA. While not eliminating the use of protective garments completely, the use of NSS may permit the use of lightweight protective garments that can perhaps reduce the prevalence of spinal disc damage among cardiologists requiring long-term wearing of PPE.

Author Contributions All authors contributed to the study conception and design. Data collection were performed by Negar Mirjalili, Jason Tse and James A Crowhurst. Material preparation and analysis were performed by Negar Mirjalili and Jason Tse. The first draft of the manuscript was written by Negar Mirjalili and all authors commented on previous versions of the manuscript. All authors read and approved the final manuscript.

Declarations

References

1. Klein LW, Goldstein JA, Haines D et al (2020) SCAI Multi-society Position Statement on Occupational Health Hazards of the Catheterization Laboratory: shifting the paradigm for Healthcare Workers' Protection. J Am Coll Cardiol 75(14):1718–1724
2. Moore B, VanSonnenberg E, Casola G et al (1992) The relationship between back pain and lead apron use in radiologists. AJR Am J Roentgenol. 158(1):191-193
3. Ross AM, Segal J, Borenstein D et al (1997) Prevalence of spinal disc disease among interventional cardiologists. Am J Cardiol 79(1):68-70
4. Goldstein JA, Balter S, Cowley M et al (2004) Occupational hazards of interventional cardiologists: prevalence of orthopedic health problems in contemporary practice. Catheter Cardiovasc Interv 63(4):407–411
5. Savage C, Seale IVTM, Shaw CJ et al (2013) Evaluation of a suspended personal Radiation Protection System vs. Conventional Apron and Shields in Clinical Interventional procedures. Open J Radiol 03:143–151
6. Wilson R, Gainor J, Valeti U et al (2018) TCT-248 a New device to markedly reduce Cardiac Cath Lab Radiation levels. J Am Coll Cardiol 72(13Supplement):B103–B103
7. Dixon SR, Rabah M, Emerson S et al (2022) A novel catheterization Laboratory Radiation Shielding System: results of pre-clinical testing. Cardiovasc Revascularization Med 36:51–55
8. Scott H, Gallagher S, Abbott W et al (2022) Assessment of occupational dose reduction with the use of a floor mounted mobile lead radiation protection shield. J Radiol Prot 42(3):033501
9. Rivett C, Dixon M, Matthews L et al (2016) An Assessment of the dose reduction of commercially available lead protective glasses for interventional Radiology Staff. Radiat Prot Dosimetry 172(4):443–452
10. Hu P, Kong Y, Chen B et al (2017) Shielding effect of lead glasses on radiologists' Eye Lens exposure in interventional procedures. Radiat Prot Dosimetry 174(1):136–140
11. McVey S, Sandison A, Sutton DG (2013) An assessment of lead eyewear in interventional radiology. J Radiol Prot 33(3):647–659
12. Van Rooijen BD, De Haan MW, Das M et al (2014) Efficacy of radiation safety glasses in interventional radiology. Cardiovasc Intervent Radiol 37(5):1149–1155
13. Nicol AL, Chung BA, Benzon HT (2018) Fluoroscopy and Radiation Safety. In Benzon HT, Raja SN, Liu SS, Fishman SM, Cohen SP (eds) Essentials of Pain Medicine, 4th edn. Elsevier, pp 703-714